Journal of Alloys and Compounds 792 (2019) 116–121

Contents lists available at ScienceDirect

Journal of Alloys and Compounds

journal homepage: http://www.elsevier.com/locate/jalcom

Deviatoric deformation kinetics in high entropy alloy under hydrostatic compression

E-Wen Huang [a, *], Chih-Ming Lin [b, **], Jenh-Yih Juang [c, ***], Yao-Jen Chang [d], Yuan-Wei Chang [a], Chan-Sheng Wu [d], Che-Wei Tsai [d, e], An-Chou Yeh [d, e], Sean R. Shieh [f], Ching-Pao Wang [f], Yu-Chun Chuang [g], Yen-Fa Liao [g], Dongzhou Zhang [h], Tony Huang [i], Tu-Ngoc Lam [a], Yi-Hung Chen [a]

[a] Department of Materials Science and Engineering, National Chiao Tung University, 1001 University Road, Hsinchu, 30010, Taiwan, ROC
[b] Department of Physics, National Tsing Hua University, Hsinchu, 30013, Taiwan, ROC
[c] Department of Electrophysics, National Chiao Tung University, Hsinchu, 30010, Taiwan, ROC
[d] Department of Materials Science and Engineering, National Tsing Hua University, Hsinchu, 30013, Taiwan, ROC
[e] High Entropy Materials Center, National Tsing Hua University, Hsinchu, 30013, Taiwan, ROC
[f] Department of Earth Sciences, University of Western Ontario, London, ON, N6A 5B7, Canada
[g] National Synchrotron Radiation Research Center, Hsinchu, 30076, Taiwan, ROC
[h] Partnership for Extreme Crystallography, University of Hawaii at Manoa, Honolulu, HI, 96822, USA
[i] Department of Earth Sciences, National Cheng Kung University, Tainan, 701, Taiwan, ROC

ARTICLE INFO

Article history:
Received 3 December 2018
Received in revised form
5 March 2019
Accepted 25 March 2019
Available online 29 March 2019

Keywords:
High pressure
High entropy alloys
Cantor alloy
Phase transformation

ABSTRACT

An equiatomic CoCrFeMnNi high-entropy alloy under hydrostatic compression is investigated using *in-situ* angular-dispersive X-ray diffraction to explore the polymorphism in high entropy alloy systems. The metallic system is of face-centered-cubic structure at ambient condition and applied hydrostatic pressures up to 20 GPa via diamond anvil cell. The angle-resolved diffraction-intensity evolutions of multiple diffraction peaks were collected simultaneously to elucidate the phase stability examinations. The phase transformation from face-centered-cubic to hexagonal-close-packed structure was evidently observed in CoCrFeMnNi alloy accompanied by a deviatoric strain subjected to the hydrostatic compression. We found lattice-asymmetric crossover before and after the phase transformation subjected to hydrostatic compression surroundings. Deviatoric strain triggers fcc-hcp phase transformation as local heterogeneity-driven lattice distortion is significant for CoCrFeMnNi alloy.

1. Introduction

Underlying mechanisms governing phase transformation in the high entropy alloys have received extensive attention. Transformation-induced plastic deformation [1] and polymorphism [2] had been reported. However, the basic thermodynamics principles and atomistic mechanisms that give rise to the phase transformation in high entropy alloys are still controversial to date [3,4]. Specifically, multiple driving forces have been estimated and compared to evaluate whether the high entropy alloys are at thermionically stable or metastable [5,6]. Nevertheless, the kinetics of phase transformation in high entropy alloys remains largely unexplored. Typically, the phase transformation driven by a temperature change, either from one single-phase to another one or from one to other multiple phases, is mainly subjected to the reaction direction toward equilibrium. Gibbs free energy summarizes the phase transformation from the effects of interface, surface, volume, and strain energies for solidification and diffusional transformation in solids, such as precipitation [7]. Another type of phase transformation is the diffusionless displacive transformation. The most famous example of this type of phase transformation is the martensitic transformation in steels, where it has been well established that the content of carbon in steel can change the habit plane for the phase transformation [8]. In such a case, the deformation kinetics typically involves shearing, such as Bain strain [9].

* Corresponding author.
** Corresponding author.
*** Corresponding author.
E-mail addresses: ewhuang@g2.nctu.edu.tw (E.-W. Huang), cm_lin@phys.nthu.edu.tw (C.-M. Lin), jyjuang@cc.nctu.edu.tw (J.-Y. Juang).

https://doi.org/10.1016/j.jallcom.2019.03.349

Most of the displacive phase transformations are characterized by crystallographic rearrangement, such as from the face-centered-cubic (fcc) structured austenite into body-centered tetragonal (bct) structured martensite, with a tremendous amount of accompanying shear deformation parallel to the habit plane together with complementary dilation [10].

Niu et al. [11] reported that, in the CoCrFeMnNi high-entropy alloy, there is a fcc to hexagonal-close-packed (hcp) phase transformation occurring in the necking regions of tensile specimens where the largest plastic deformation is expected. Their atomistic models and transmission electron microscopy (TEM) analyses revealed that shear deformation triggered the ABCABC type stacking in fcc structure to the ABABAB stacking hcp structure on the closed-packed planes. This type of phase transformation is achieved by forming Shockley partial dislocations generated by shearing [11] and, thus, is diffusionless similar to that of the martensitic transformation in the steels.

On the other hand, similar fcc to hcp phase transformations had been reported in high entropy alloys albeit that, in those cases, the transformation was induced by the hydrostatic compression instead of severe tensile strain as described above [2,12,13]. The deformation on lattice resulting from quasi-hydrostatic compression is very different from that arising from non-hydrostatic deformation. Bell and Mao have shown that when the nearly hydrostatic conditions are achieved using helium as a pressure transmitting medium, the lattice parameters can be measured by energy dispersive synchrotron radiation [14]. Speziale et al. [15] pointed out that the non-hydrostatic deformation could induce anisotropic deformation for different crystallographic orientations. In principle, the hydrostatic compression confines volume changes of the system with isotropic deformation.

However, as mentioned above, shearing and crystallographic anisotropic deformation are playing important roles in both the reported fcc to hcp phase transformation in CoCrFeMnNi high entropy alloys [11] and martensitic phase transformation in steels [8–10,16]. For the equiatomic medium- [17] and high-entropy [18,19] alloys, Niu et al. proposed that the chemistry and magnetic properties of the constituent alloy elements might lead to phase transformation triggered by dislocation slip and its interaction with internal boundaries [11].

For steels, chemistry also plays an important role, such as tuning the stacking-fault energy for the phase transformation [20]. In this respect, manganese is known for its role for twinning-induced plasticity for deformation [21,22], anisotropy of elasticity [23], creep [24], magnetic properties [25], and magnetocaloric effect [21,26] in various material systems. Hence, the focus of this report is to control the manganese content of the high entropy alloys to study its effects on hydrostatic compression-induced phase transformation by using the *in-situ* angle-dispersive synchrotron x-ray diffraction measurements.

2. Experiment

In this study, two different high entropy alloys were prepared. One is the Cantor alloys, which had been reported to exhibit the fcc to hcp phase transformation when subjected to tension [11] and hydrostatic compression [2,12,13], respectively. The other is the $Al_{0.3}CoCrCu_{0.3}FeNi$ high-entropy alloy, which will serve as a reference because aluminum is known for its high stacking fault energy (~166–200 mJ/m^2) [27,28].

Our methodology is briefly described in the following. We assume that both the fcc and hcp phase lattice can be formed by stacking closed-packed layers. If a dislocation with a Burgers vector $\frac{a}{6}[1\ 1\ \bar{2}]$ glide between two (1 1 1) layers of a fcc lattice, all layers will be shifted. Therefore, all atoms above the glide plane occupying different sites as the Shockley partial dislocation and causing a stacking fault. This fault can convert the lattice stacking into a hexagonal close-packed sequence, resulting in a glissile interface separating the adjacent fcc and hcp phases. Based on this assumption, the main purpose of the present study is to experimentally verify the pressure-induced phase transition by characterizing crystallographic features as a function of applied pressure using the *in-situ* angle dispersive x-ray diffraction (ADXRD). The details of *in-situ* high-pressure experimental methods are archived in our earlier work [13]. It is expected that such experiments would provide solid evidences indicating features, such as the paths leading fcc to hcp, as well as the texture development and anisotropic lattice deformation. Moreover, our hypothesis may be further validated by experimentally identifying that the fcc-hcp transformation is indeed occurring upon the planar coherent facets of (0 0 0 1).

3. Results and discussion

Fig. 1 is the azimuthally-resolved diffraction map to comparing the intensity evolution subjected to applied stress. The x-axis and y-axis of the Cartesian coordinates shown in Fig. 1 are the reciprocal space ($\frac{1}{\text{Å}}$) and azimuthal angle, respectively. Fig. 1(a) is for the stress at 1.35 GPa. Similarly, Fig. 1(b) is for 3.78 GPa; (c) for 5.36 GPa; (d) for 6.78 GPa; (e) for 7.10 GPa; (f) for 7.26 GPa; (g) for 8.53 GPa; (h) for 9.17 GPa; (i) for 9.80 GPa; (j) for 11.89 GPa; (k) for 14.14 GPa; (l) for 17.06 GPa; (m) for 20.00 GPa, and (n) for decompression to 10.44 GPa, respectively. The (1 1 1) and (2 0 0) diffraction peaks of fcc and the (1 0 0 0), (0 0 0 2), and (1 0 $\bar{1}$ 1) peaks of hcp are marked, respectively. For the convenience of comparison, the maximum and minimum of the intensity are set to be identical for Fig. 1(a)~(n) and 1(p). Fig. 1(o) shows the integrated diffraction patterns of the CoCrFeMnNi high entropy alloy after relaxation from high-pressure measurements to ambient.

The X-ray diffraction features have been applied to characterize the hcp crystals for texture development [29,30]. The (1 0 0 0), (0 0 0 2), and (1 0 $\bar{1}$ 1) diffractions are marked in Fig. 1(o) to illustrate that the majority of the system is indeed a hcp phase. We follow Kanitpanyacharoen et al.'s methods [29,30] to resolve the orientation-dependent diffraction intensity in azimuthal angles to examine hcp phase as shown in Fig. 1(p). The sinusoidal variations in peak positions are a result of deviatoric stress. The variation in intensity along the diffraction rings indicates a crystallographic preferred orientation attained subjected to plastic deformation.

Specifically, the intensity maxima of the (0 0 0 2) diffraction peaks are highlighted and marked in Fig. 1(p) as $3.13\frac{1}{\text{Å}}$ with the azimuthal angle of 200° and 163°, respectively. Similarly, the intensity maxima of (1 0 $\bar{1}$ 1) diffraction peaks are highlighted and marked in Fig. 1(p) as $3.30\frac{1}{\text{Å}}$ with the azimuthal angle locating at 267° and at 93°, respectively. Fig. 1(q)~(s) are simplified illustrations showing phase-ratio evolution. Niu et al. [11]'s simulation and our earlier experimental evidence [13] show more details of possible deformation paths involving stacking faults.

Deformation mechanisms for hcp metals are well established and concluded as either being dominated by the basal and prismatic slips or by twinning induced by tensile and compressive strains [31–33]. In particular, mechanical twinning and shearing have been found to play important roles in texture development for hcp-structured metals. Mechanical twinning is unidirectional and characterized as tensile or compressive strain parallel to the c-axis. Here, we follow the conventional descriptions of the twinning modes as tensile twinning and compressive twinning, but not the mode of deformation in our experiment.

For the hcp crystal structure with a specific c/a ratio, the angle between (0 0 0 1): (1 0 $\bar{1}$ 1) = $tan^{-1}\left(2c/\sqrt{3}a\right)$, where a and c are

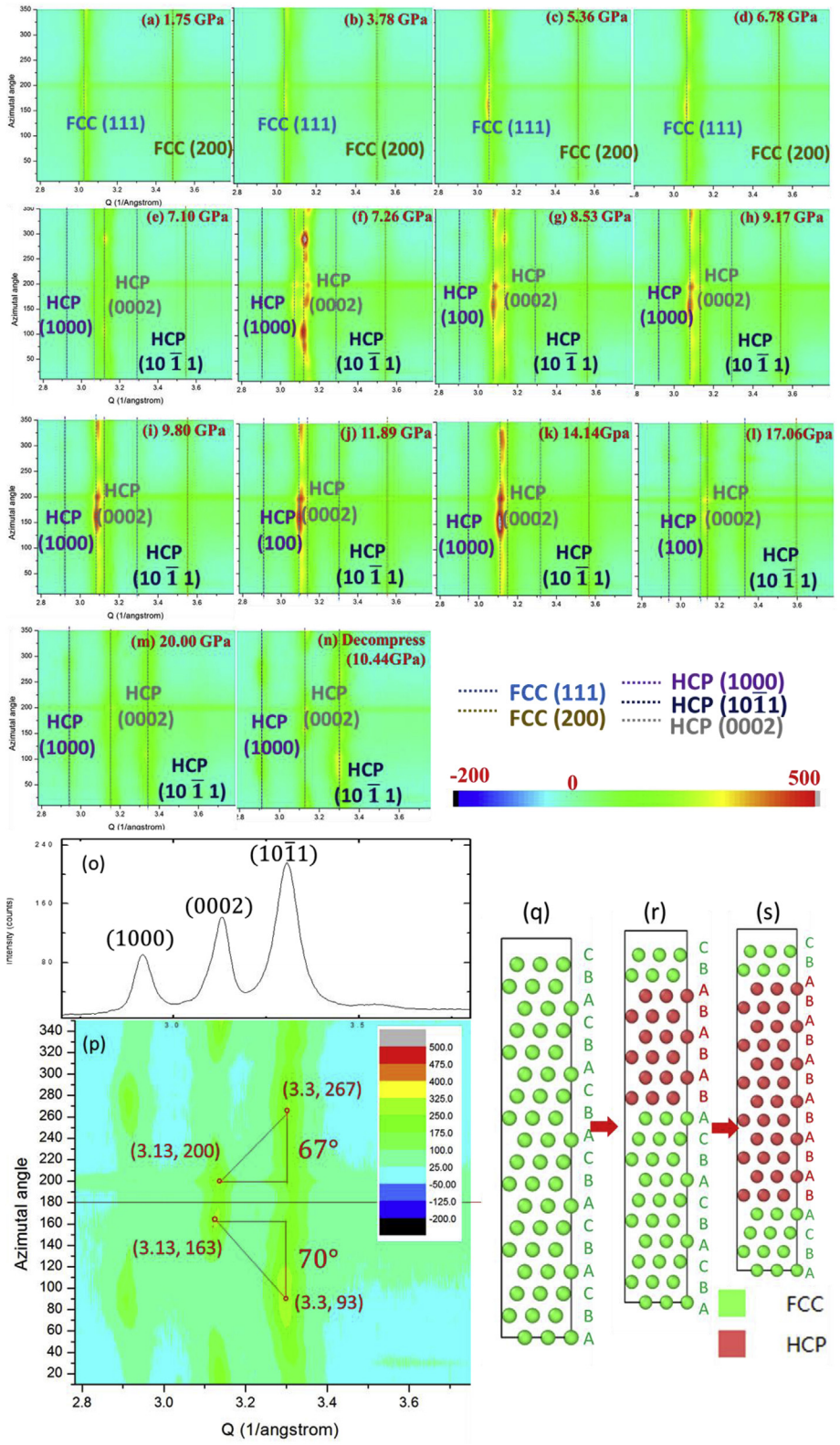

Fig. 1. Diffraction results of the system collected subjected to hydrostatic compression: **(a)~(m); (n)** after decompression. After relaxation to ambient: (o) Integrated peaks showing the majority of the phase is hcp as marked by hcp peaks of (1 0 $\bar{1}$ 0), (0 0 0 2), and (1 0 $\bar{1}$ 1). (p) Azimuthally-resolved results. The intensity is colored as contour map. (q)~(s) are schematic illustration.

the lattice parameters used in the usual hcp lattice, respectively. The angle for orientations of (0 0 0 2) at azimuthal angles 200° and of (1 0 $\bar{1}$ 1) at azimuthal angles 267° is 67°. The angle for orientations of (0 0 0 2) at azimuthal angles 163° and of (1 0 $\bar{1}$ 1) at azimuthal angles 93° is 70°. Comparing to zinc with the hcp crystal structure, the (0 0 0 1): $(1\,0\,\bar{1}\,1) = tan^{-1}\left(2c/\sqrt{3}a\right) = 67°$ would lead to a c/a ratio equals to 1.86.

The integrated diffraction peaks of the hcp phase were used to estimate the lattice parameters a and c as a function of the applied stress, as well. The results are displayed in Fig. 2(a) with a and c being denoted as circles (○) and triangles (△), respectively. The change of lattice constant a on the basal plane of the hcp phase shows essentially a monotonic decrease upon compression. In contrast, the lattice constant c apparently exhibits much more fluctuations as a function of the applied compressive stress. The c/a ratio as a function of the applied pressure is shown in Fig. 2(b). The fluctuations of lattice constant c are magnified in Fig. 2(b) as compared to that displayed in Fig. 2(a). Note that the c/a ratio of CoCrFeMnNi is always smaller than 1.732 ($\cong\sqrt{3}$), indicating that the deformation mode is dominated by the tensile twinning similar to that for Zn [29,30].

The characteristic twinning shear for a particular twin system depends on the c/a axial ratio. It relates the amount of shear contributed by the twin system to the volume fraction of the grain that reorients by twinning. Kanitpanyacharoen et al.'s visco-plastic self-consistent (VPSC) polycrystal plasticity model suggests that the gradual texture evolution observed in zinc is controlled primarily by (0 0 0 1) <2 $\bar{1}$ $\bar{1}$ 0> basal slip and subsequently accompanied by (1 0 $\bar{1}$ 2) <$\bar{1}$ 0 1 1> tensile twinning when the c/a ratio is below 1.732 ($\cong\sqrt{3}$) [29,30].

Considering the effect of partial dislocation $\frac{a}{6}[1\,1\,\bar{2}]$ gliding between layers of fcc and hcp, the sequence of Shockley partial dislocations may be activated along the (1 1 1) of fcc phase and creates glissile interface separating the fcc from hcp phases. The fluctuations of the c-axis parameter may, thus, reflect the activities of the diffusionless phase-transformation kinetics.

Besides the deformation of the hcp phase, there is concurrent deformation of the fcc phase in the system. It is noted that, in the diffraction results, there are many diffraction peaks arising from the fcc phase superimposing that of the hcp phase. To distinguish the deformation behavior in the fcc phase from that prevailing in the hcp phase, the (2 0 0) peak of the fcc phase is selected, because it does not superimpose with other hcp peaks. The (2 0 0) lattice-strain evolution is shown in Fig. 3. The azimuthal-angle resolved results are presented as a function of applied compressive stress. Different colors show different levels of the compressive strains of the fcc (2 0 0). The dark blue color (■) shows lower compressive lattice strain at smaller applied stress prior to the phase transformation. Comparing to the other lattice strain distribution subjected to higher applied stresses, the dark blue color region is relatively uniform, indicating the feature of isotropic deformation. However, there is an obvious nonuniform lattice strain distribution shown in the distorted contour in Fig. 3. In Fig. 3, when the stress is greater than 4 GPa, there is anisotropic lattice deformation. Anisotropic deformation along different orientations can introduce local shear. Consequently, the anisotropic lattice shear shown in Fig. 3 could be the origin of the deviatoric strains for the fcc-hcp phase transformation as well as the driving force for the collective displacive phase transformation at atomic levels.

The complementary diffraction intensity, lattice-strain, and peak-width evolutions for both of the fcc and hcp phases are shown in Fig. 4. Fig. 4(a) is the evolution of integrated intensity for Q covering both fcc (1 1 1) and hcp (0 0 0 2) peaks; (b) is for fcc (2 0 0) peak, and (c) is for hcp (1 0 $\bar{1}$ 1) peak. Fig. 4(d) and (e) for fcc lattice-strain evolutions of (2 0 0) and (1 1 1), respectively. Fig. 4(f) and (g) for hcp lattice-strain evolutions of (1 0 $\bar{1}$ 1) and (0 0 0 2). The hcp (0 0 0 2) lattice-strain evolution shows most anisotropy in azimuthal

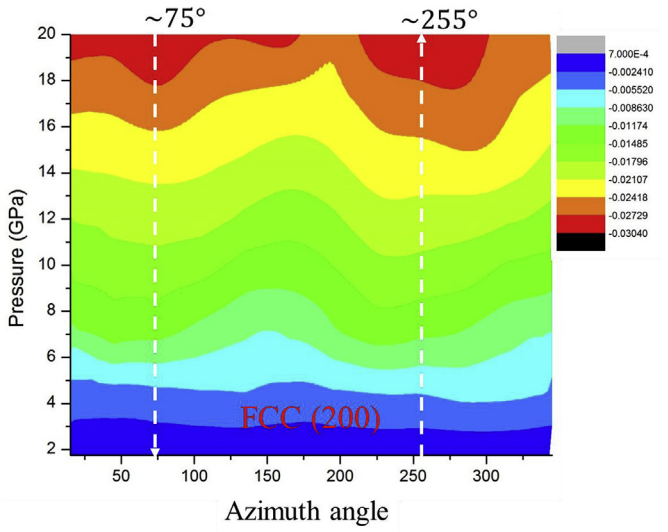

Fig. 3. Azimuthal-resolved lattice strain (e) evolution of FCC (200) peaks as a function of applied hydrostatic compressive stresses.

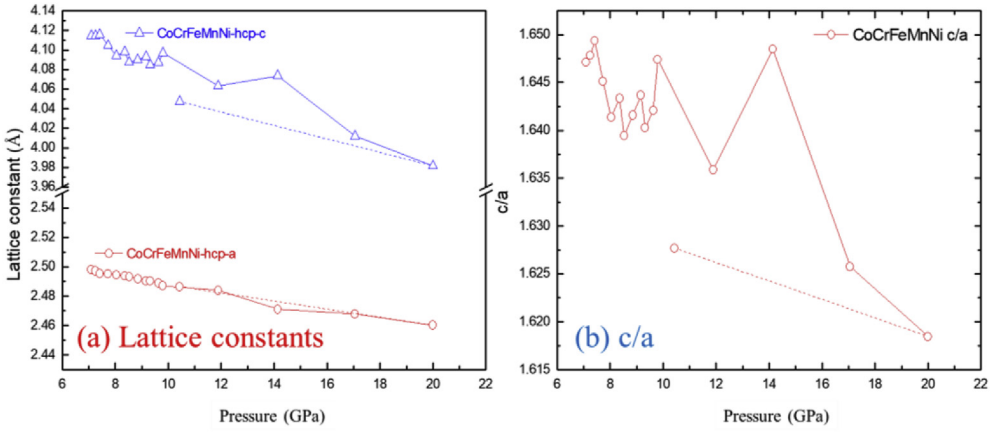

Fig. 2. (a) Lattice-constant evolutions of c (○) and a (△), respectively. (b) The c/a ratio.

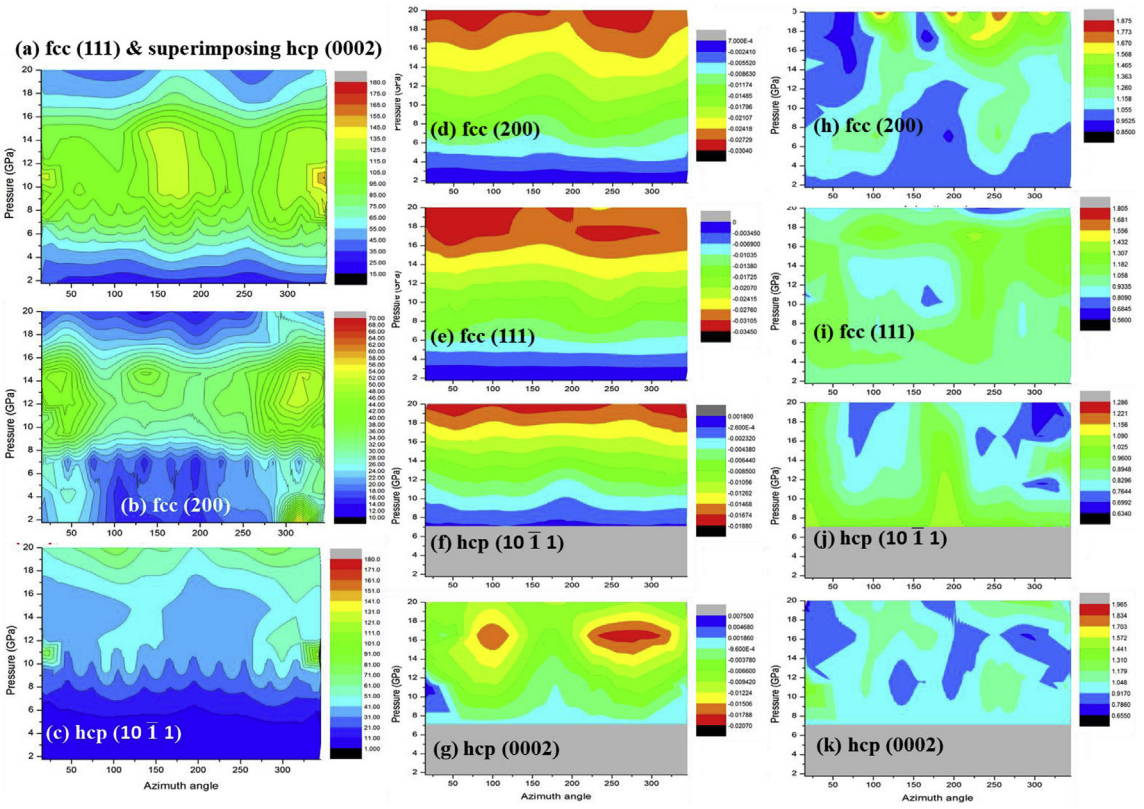

Fig. 4. Intensity, lattice-strain, and peak-width evolution of fcc and hcp phases. (a) Integrated intensity covering fcc (1 1 1) and hcp (0 0 0 2) peaks; (b) fcc (2 0 0) intensity; (c) hcp (1 0 $\bar{1}$ 1) intensity. Lattice strain, unit is e: (d) fcc (2 0 0); (e) fcc (1 1 1); (f) hcp (1 0 $\bar{1}$ 1); (g) hcp (0 0 0 2). Full-width-at-half-maximum (FWHM): (h) fcc (2 0 0); (i) fcc (1 1 1); (j) hcp (1 0 $\bar{1}$ 1); (k) hcp (0 0 0 2).

angles where most compression shown at azimuthal angles centered around 90° and 270°, respectively. The possible mechanisms have been discussed above as twinning activities similar to Zn [29,30].

Fig. 4(h) and (i) for fcc peak-width evolutions in the full-width-at-half-maximum (FWHM) of diffraction peaks of (2 0 0) and (1 1 1), respectively. Fig. 4(f) and (g) for hcp peak-width evolutions of (1 0 $\bar{1}$ 1) and (0 0 0 2). The changes of peak widths indicate the dislocation evolution upon the shear deformation and the phase transformation. Referring to Kanitpanyacharoen et al.'s polycrystal plasticity model, the features shown in Fig. 4 reveal the dominant deformation mode in the CoCrFeMnNi high entropy alloy could be the twinning-assisted phase transformation, which is more close to Path 3 of Niu et al.'s simulation [11].

Wang et al.'s in-situ high-pressure synchrotron radiation X-ray diffraction measurements also show abundant polymorphic transitions in the $Al_{0.6}$CoCrFeNi high-entropy alloy. The original body-centered cubic (bcc) phase transfers to an orthorhombic phase at ~ 10.6 GPa during compression at room temperature, and the orthorhombic phase remains stable up to ~ 40 GPa [34]. Our reference system of $Al_{0.3}CoCrCu_{0.3}FeNi$ high entropy alloys are shown in the supplementary results as S.1. Unlike Wang et al.'s $Al_{0.6}$CoCrFeNi high-entropy alloy in bcc structure [34], our reference system also contains Al, but has Cu, is in fcc structure. It is evident that all the features suggesting anisotropic lattice deformation or even texture development are absent in our fcc $Al_{0.3}CoCrCu_{0.3}FeNi$ high entropy alloys. The present results thus clearly illustrate the prominent role played by the manganese in facilitating the deviatoric deformation and accompanying fcc-to-hcp phase transition in the CoCrFeMnNi high entropy alloys.

There is also a possibility of grain-size effect that might cause the inhomogeneous and deviatoric results. Specifically, Zhang et al.'s summarize the effects of non-hydrostaticity and grain size on the pressure-induced phase transition of the CoCrFeMnNi high-entropy alloy [35]. Another possibility is the magnetically-driven transformation as Huang et al.'s prediction [5] and Niu et al.'s simulation [11]. Our findings emphasize the fact that the polymorphism of high entropy alloys is sensitive to multi-scale microstructures. The critical parameters involve magnetics, elements, crystal structure, stacking faults, and twinning. An important finding is that hydrostatic surrounding on high entropy alloys can trigger local shear. These results provide experimental evidences for manufacturing and tuning the metastable structures of the high entropy alloys.

4. Conclusion

In conclusion, in this work we present an orientation-resolved diffraction distribution to quantify the pressure-dependent lattice parameters of *a* and *c*, for the structural evolution of the CoCrFeMnNi high entropy alloy under quasi hydrostatic compression. Our results showed that, for the hexagonal-close-packed phase, the *c*/*a* ratio changes more or less monotonically with the increasing applied hydrostatic compression with the *c*/*a* ratio being always smaller than 1.732 ($\cong\sqrt{3}$). Moreover, the proposed deformation model is further verified by the anisotropic lattice straining and induced local shearing observed in the diffraction results. The major contribution of the present work is that it provides an alternative perspective to look into the deformation modes of various high entropy alloy systems by high-pressure experiments.

Acknowledgement

The authors are grateful to the support of "High Entropy Materials Center", National Tsing Hua University and "Center for Semiconductor Technology Research" from The Featured Areas Research Center Program within the framework of the Higher Education Sprout Project by the Ministry of Education (MOE) in Taiwan, and the Ministry of Science and Technology (MOST) Programs 107-2218-E-007-012, 107-3017-F-009-002, and 107-3017-F-007-003. CML and JYJ are supported by MOST of Taiwan under grant #: 106-2112-M-009-013-MY3. YWC and CML appreciate the technical supports from GeoSoilEnviroCARS, Argonne National Laboratory, APS BL13BMC, SPring8 BL12B1, NSRRC BL01C. EWH, TNL, and YHC are supported by MOST 104-2628-E-009-003-MY3 and 107-2628-E-009-001-MY3.

Appendix A. Supplementary data

Supplementary data to this article can be found online at https://doi.org/10.1016/j.jallcom.2019.03.349.

Disclosure statement

No potential conflict of interest was reported by the authors.

References

[1] Z.M. Li, K.G. Pradeep, Y. Deng, D. Raabe, C.C. Tasan, Metastable high-entropy dual-phase alloys overcome the strength-ductility trade-off, Nature 534 (2016) 227–+.
[2] F. Zhang, Y. Wu, H.B. Lou, Z.D. Zeng, V.B. Prakapenka, E. Greenberg, Y. Ren, J.Y. Yan, J.S. Okasinski, X.J. Liu, Y. Liu, Q.S. Zeng, Z.P. Lu, Polymorphism in a high-entropy alloy, Nat. Commun. 8 (2017).
[3] D.B. Miracle, O.N. Senkov, A critical review of high entropy alloys and related concepts, Acta Mater. 122 (2017) 448–511.
[4] Y. Zhang, T.T. Zuo, Z. Tang, M.C. Gao, K.A. Dahmen, P.K. Liaw, Z.P. Lu, Microstructures and properties of high-entropy alloys, Prog. Mater. Sci. 61 (2014) 1–93.
[5] S. Huang, W. Li, S. Lu, F. Tian, J. Shen, E. Holmström, L. Vitos, Temperature dependent stacking fault energy of FeCrCoNiMn high entropy alloy, Scripta Mater. 108 (2015) 44–47.
[6] Y.H. Zhang, Y. Zhuang, A. Hu, J.J. Kai, C.T. Liu, The origin of negative stacking fault energies and nano-twin formation in face-centered cubic high entropy alloys, Scripta Mater. 130 (2017) 96–99.
[7] D.A. Porter, K.E. Easterling, M.Y. Sherif, Phase Transformations in Metals and Alloys, CRC Press, Boca Raton, FL, 2009.
[8] G. Krauss, Martensite in steel: strength and structure, Mater. Sci. Eng. A 273–275 (1999) 40–57.
[9] L. Qi, A.G. Khachaturyan, J.W. Morris, The microstructure of dislocated martensitic steel: Theory, Acta Mater. 76 (2014) 23–39.
[10] D.D. Tjahjanto, S. Turteltaub, A.S.J. Suiker, Crystallographically based model for transformation-induced plasticity in multiphase carbon steels, Continuum Mech. Therm. 19 (2008) 399–422.
[11] C. Niu, C.R. LaRosa, J. Miao, M.J. Mills, M. Ghazisaeidi, Magnetically-driven phase transformation strengthening in high entropy alloys, Nat. Commun 9 (2018) 1363.
[12] C.L. Tracy, S. Park, D.R. Rittman, S.J. Zinkle, H. Bei, M. Lang, R.C. Ewing, W.L. Mao, High pressure synthesis of a hexagonal close-packed phase of the high-entropy alloy CrMnFeCoNi, Nat. Commun. 8 (2017) 15634.
[13] E.W. Huang, C.-M. Lin, J. Jain, S.R. Shieh, C.-P. Wang, Y.-C. Chuang, Y.-F. Liao, D.-Z. Zhang, T. Huang, T.-N. Lam, W. Woo, S.Y. Lee, Irreversible phase transformation in a CoCrFeMnNi high entropy alloy under hydrostatic compression, Mater. Today Commun. 14 (2018) 10–14.
[14] H.K. Mao, P.M. Bell, Carnegie Inst. Wash. Yearb. 80 (1981), 404-404.
[15] S. Speziale, C.S. Zha, T.S. Duffy, R.J. Hemley, H.K. Mao, Quasi-hydrostatic compression of magnesium oxide to 52 GPa: implications for the pressure-volume-temperature equation of state, J. Geophys. Res. Solid Earth 106 (2001) 515–528.
[16] H. Beladi, G.S. Rohrer, A.D. Rollett, V. Tari, P.D. Hodgson, The distribution of intervariant crystallographic planes in a lath martensite using five macroscopic parameters, Acta Mater. 63 (2014) 86–98.
[17] B. Gludovatz, A. Hohenwarter, K.V.S. Thurston, H. Bei, Z. Wu, E.P. George, R.O. Ritchie, Exceptional damage-tolerance of a medium-entropy alloy CrCoNi at cryogenic temperatures, Nat. Commun. 7 (2016) 10602.
[18] B. Gludovatz, A. Hohenwarter, D. Catoor, E.H. Chang, E.P. George, R.O. Ritchie, A fracture-resistant high-entropy alloy for cryogenic applications, Science 345 (2014) 1153–1158.
[19] J.W. Yeh, S.K. Chen, S.J. Lin, J.Y. Gan, T.S. Chin, T.T. Shun, C.H. Tsau, S.Y. Chang, Nanostructured high-entropy alloys with multiple principal elements: novel alloy design concepts and outcomes, Adv. Eng. Mater. 6 (2004) 299–303.
[20] A. Dumay, J.P. Chateau, S. Allain, S. Migot, O. Bouaziz, Influence of addition elements on the stacking-fault energy and mechanical properties of an austenitic Fe-Mn-C steel, Mater. Sci. Eng. Struct. Mater. Prop. Microstruct. Process. 483–84 (2008) 184–187.
[21] P. Chowdhury, D. Canadinc, H. Sehitoglu, On deformation behavior of Fe-Mn based structural alloys, Mater. Sci. Eng. R Rep. 122 (2017) 1–28.
[22] K.H. Kwon, J.S. Jeong, J.K. Choi, Y.M. Koo, Y. Tomota, N.J. Kim, In-situ neutron diffraction analysis on deformation behavior of duplex high Mn steel containing austenite and epsilon-martensite, Met. Mater. Int. 18 (2012) 751–755.
[23] E.-W. Huang, D. Yu, J.-W. Yeh, C. Lee, K. An, S.-Y. Tu, A study of lattice elasticity from low entropy metals to medium and high entropy alloys, Scripta Mater. 101 (2015) 32–35.
[24] W. Woo, E.-W. Huang, J.-W. Yeh, H. Choo, C. Lee, S.-Y. Tu, In-situ neutron diffraction studies on high-temperature deformation behavior in a CoCrFeMnNi high entropy alloy, Intermetallics 62 (2015) 1–6.
[25] T. Erika, C. Sebastian, Z. Fernando, D. Veronica, Temperature performance of AB(5) hydrogen storage alloy for Ni-MH batteries, Int. J. Hydrogen Energy 41 (2016) 19684–19690.
[26] V. Verma, A. Tripathi, K.N. Kulkarni, On interdiffusion in FeNiCoCrMn high entropy alloy, J. Phase Equilib. Diffus. 38 (2017) 445–456.
[27] Y. Mishin, D. Farkas, M.J. Mehl, D.A. Papaconstantopoulos, Interatomic potentials for monoatomic metals from experimental data and ab initio calculations, Phys. Rev. B 59 (1999) 3393–3407.
[28] W.R. Tyson, W.A. Miller, Surface free energies of solid metals - estimation from liquid surface-tension measurements, Surf. Sci. 62 (1977) 267–276.
[29] W. Kanitpanyacharoen, S. Merkel, L. Miyagi, P. Kaercher, C.N. Tome, Y. Wang, H.R. Wenk, Significance of mechanical twinning in hexagonal metals at high pressure (vol 60, pg 430, 2012), Acta Mater. 137 (2017), 124-124.
[30] W. Kanitpanyacharoen, S. Merkel, L. Miyagi, P. Kaercher, C.N. Tomé, Y. Wang, H.R. Wenk, Significance of mechanical twinning in hexagonal metals at high pressure, Acta Mater. 60 (2012) 430–442.
[31] J.W. Christian, S. Mahajan, Deformation twinning, Prog. Mater. Sci. 39 (1995) 1–157.
[32] J. Jain, W.J. Poole, C.W. Sinclair, M.A. Gharghouri, Reducing the tension-compression yield asymmetry in a Mg-8Al-0.5Zn alloy via precipitation, Scripta Mater. 62 (2010) 301–304.
[33] H. Wang, S.Y. Lee, M.A. Gharghouri, P.D. Wu, S.G. Yoon, Deformation behavior of Mg-8.5wt.%Al alloy under reverse loading investigated by in-situ neutron diffraction and elastic viscoplastic self-consistent modeling, Acta Mater. 107 (2016) 404–414.
[34] L. Wang, F. Zhang, Z. Nie, F. Wang, B. Wang, S. Zhou, Y. Xue, B. Cheng, H. Lou, X. Chen, Y. Ren, D.E. Brown, V. Prakapenka, E. Greenberg, Z. Zeng, Q.S. Zeng, Abundant polymorphic transitions in the Al 0.6 CoCrFeNi high-entropy alloy, Mater. Today Phys. 8 (2019) 1–9.
[35] F. Zhang, H. Lou, C. Songyi, X. Chen, Z. Zeng, J. Yan, W. Zhao, Y. Wu, Z. Lu, Q.S. Zeng, Effects of non-hydrostaticity and grain size on the pressure-induced phase transition of the CoCrFeMnNi high-entropy alloy, J. Appl. Phys. 124 (2018) 115901.